Development of High Shrinkage Polyethylene Terephthalate (PET) Shape Memory Polymer Tendons for Concrete Crack Closure

Oliver Teall[1]; Martins Pilegis[2]; John Sweeney[3]; Tim Gough[4]; Glen Thompson[5]; Anthony Jefferson[6]; Robert Lark[7]; Diane Gardner[8]

[1]*Cardiff University School of Engineering, Queen's Buildings, The Parade, Cardiff CF24 3AA*

[2]*Cardiff University School of Engineering, Queen's Buildings, The Parade, Cardiff CF24 3AA*

[3]*Bradford University School of Engineering, Bradford, West Yorkshire, BD7 1DP*

[4]*Bradford University School of Engineering, Bradford, West Yorkshire, BD7 1DP*

[5]*Bradford University School of Engineering, Bradford, West Yorkshire, BD7 1DP*

[6]*Cardiff University School of Engineering, Queen's Buildings, The Parade, Cardiff CF24 3AA*

[7]*Cardiff University School of Engineering, Queen's Buildings, The Parade, Cardiff CF24 3AA*

[8]*Cardiff University School of Engineering, Queen's Buildings, The Parade, Cardiff CF24 3AA*

Correspondence to: Tony Jefferson (Email: JeffersonAD@cardiff.ac.uk)

ABSTRACT

The shrinkage force exerted by restrained shape memory polymers can potentially be used to close cracks in structural concrete. This paper describes the physical processing and experimental work undertaken to develop high shrinkage die-drawn Polyethylene Terephthalate (PET) shape memory polymer tendons for use within a crack closure system. The extrusion and die-drawing procedure used to manufacture a series of PET tendon samples is described. The results from a set of restrained shrinkage tests, undertaken at differing activation temperatures, are also presented along with the mechanical properties of the most promising samples.

The stress developed within the tendons is found to be related to the activation temperature, the cross-sectional area and to the draw rate used during manufacture. Comparisons with commercially-available PET strip samples used in previous research are made, demonstrating an increase in restrained shrinkage stress by a factor of two for manufactured PET filament samples.

1 INTRODUCTION

Shape Memory Polymers (SMPs) alter their physical shape in response to various stimuli, such as a change in heat, light (UV and infrared) or chemical concentration (e.g. moisture, pH).[1-3]

The simplest type of SMP is formed from amorphous polymer. In this case the SMP is created

by heating the material to a temperature above the glass transition temperature (T_g), inducing molecular chain orientation by stretching it, and then freezing in the orientation by cooling. The orientation can be released at a later time by increasing the temperature to a trigger temperature, which is at or above T_g, at which point the material reverts wholly or partially to its pre-oriented shape. Other types of SMP can be formed from semi-crystalline polymer, in which case the stretching and trigger temperatures will be governed by the temperature dependence of the mechanical properties of the crystals. Similar macroscopic physical behaviour can be accomplished for both amorphous and semicrystalline polymer, and in either case this shape change ability can be categorised as a shape memory effect (SME).[1,2,4]

If an amorphous SMP, having been stretched into its oriented state ("programmed"), is then heated above T_g while restrained, a restrained shrinkage stress will be generated. Restrained shrinkage stresses observed in unmodified SMPs generally range from a few tenths of a megapascal (MPa) to a few tens of MPa, depending on the material and programming regime used.[2,5,6] A key parameter which determines the final stress achieved is the temperature at which the SMP has been programmed, and the maximum value for the stress upon reheating generally occurs at or near the programming temperature initially used.[3,7] The restrained shrinkage stress also depends upon the programming strain and strain rate.[3,7]

The magnitude of the restrained shrinkage stress is positively correlated with the energy stored by the SMP during deformation, and is limited by the relatively low elastic modulus of the material in the rubbery state (above T_g). Efforts to improve the rubbery state elastic modulus have included increasing the cross-linking density and the incorporation of fillers into the polymer matrix. Common fillers include carbon nanotubes (CNTs) and carbon nanofibres (CNFs), as well as glass or Kevlar fibres, carbon powders and SiC particles.[5,6] Such

inclusions have been shown to increase the recovery stress;[2] however, the associated increase in cost and T_g of the SMP would likely be a prohibiting factor within a concrete crack closure system. The focus of the experiments within this paper, therefore, is on comparing the restrained shrinkage stresses of unmodified drawn PET (in essentially amorphous form) with differing cross sections and processing methods.

In terms of thermal activation, the triggering temperature must be chosen to suit the application. Polymers may be specially formulated to produce the required activation temperatures. In this case, the upper limit to the trigger temperature is governed by the presence of setting concrete which can be damaged at temperatures above 100°C.

In amorphous polymers, the temperature for both inducing orientation and triggering shape recovery are closely related to T_g. PET has a glass transition temperature in the range 60 – 80 °C.[9] Previous work undertaken at Cardiff University suggested that the peak uniaxial shrinkage stress for drawn PET tape is achieved at 120 °C;[10] however, to ensure the system can be activated within concrete, an activation temperature of 90°C was chosen for the experiments described in this paper.

The purpose of this paper is to expand on the previous work on the use of shape memory polymer tendons as a crack closure system within concrete structural elements.[10,11] A number of other investigators have explored the use of shape memory materials for closing, or preventing, cracks in a range of other materials.[12-17] The particular interest of the current work is large structural concrete applications, for which higher shrinkage stresses than those previously observed are required for the crack closure system to be viable. The shrinkage stress value sought is of the order of 100MPa but lower values, in the range 30-50MPa, would allow the system to close early age cracks and enhance autogenous healing mechanisms.[18,19]

This paper describes some new restrained shrinkage stress experiments on a set of manufactured drawn PET samples of varying cross-section, which were undertaken with the aim of finding a higher shrinkage stress solution for use within the concrete crack closure system.

The polymer samples tested in the present investigation, with the exclusion of the commercially available PET shrink tite strips, are bespoke and have been produced at Bradford University for the purpose of assessing their potential for use within the concrete crack closure system. SMPs have never before been manufactured specifically for this purpose and maximising the polymer restrained shrinkage stress, for use within a cementitious system, is the long-term objective of the present work.

The geometry of the tendons tested, including their lengths of the elements and cross-sectional areas, were chosen to provide data relevant to the type of tendon required for typical structural elements.[19]

2 EXPERIMENTAL STUDY

An experimental study into the restrained shrinkage stress generated by both commercially available PET strips and PET filament samples produced at Bradford University of varying cross-section is now described. Details of the specimens tested are given in in TABLE 1 and an image of the cross-sections of all manufactured samples shown in Figure 2.

TABLE 1 Details of shape memory polymer samples tested

Designation	Material	Dimensions (unit)	Draw ratio	Draw rate (mm min^{-1})	Tests and repetitions	
Strips	Oriented PET[a]	0.046mm thickness 32mm width	unknown	unknown	TS1	3
					TS2	1
					TS3	10
					TS4	3
					TS5	3
Solid filament	Drawn PET	0.95mm dia.	4.0	1000	TS1	3
					TS2	1
					TS3	10
					TS4	3
					TS5	3
Filament tube	Drawn PET	0.95mm dia.	4.0	1000	TS1	1
					TS2	1
					TS3	10
					TS4	3
Tube	Drawn PET	6.61mm external dia. 2.56mm internal dia.	3.9	40 (initial)	TS1	1
					TS2	1
					TS3	1
Tube with filaments	Drawn PET	6.54mm dia.	4.0 (tube) 4.4 (filament)	40 (initial)	TS1	1
					TS2	1
					TS3	1

[a]Manufacturing details commercially sensitive

2.1 Material manufacturing details

PET solid and tube filament

For the PET solid filaments and tube filaments, a commercial grade of PET (Dow Lighter C93) was obtained in granular form. This polymer has a T_g of 78 °C according to manufacturer's figures and is recommended for injection moulding, stretch blow moulding and thermoforming. It was first made into fibres by melt extrusion. This was done using a single-screw Killion S1748 25 mm extruder operating at a screw speed of 15 rpm and a screw pressure of 30 bar. The maximum melt temperature in the extruder was 280 °C and the die head was at 270 °C. The material was extruded through a circular die of 4mm internal

115 diameter and hauled off at 5m min^{-1}. On exit from the die it was cooled in a glycerol bath at
116 room temperature. The final diameter of the cooled product was 1.8 mm.

117 The second stage of the process was to introduce molecular orientation into the fibres. The
118 technique of die-drawing was used, as described for polymers by Coates and Ward[20]. Fibre at
119 room temperature was pulled through a 1.5 m length fan-assisted oven with a controlled air
120 temperature. On exit from the oven, it entered a converging conical die with cone angle 30°
121 and final diameter 1 mm, held at a constant temperature. After the die, the fibre was gripped
122 by a caterpillar-type haul-off device operating at a constant linear speed. Since the highest
123 levels of orientation are associated with the highest haul-off speeds and lowest temperatures,
124 the caterpillar speed was set at its maximum 1 m min^{-1} (corresponding to an average axial
125 strain rate in the die of 17 s^{-1}) and both the oven and die temperatures were lowered in 1 °C
126 increments from 80 °C until stress whitening and failure of the fibre were observed at 75 °C.
127 The die temperature was then raised incrementally until satisfactory fibre was produced; the
128 final settings were thus 75 °C in the oven and 80°C in the die. After exiting the die, further
129 drawing took place during cooling between the die and the caterpillar, resulting in a final
130 diameter of 0.9 mm, corresponding to a draw ratio of 4.0. At the start of the process the haul-
131 off force was measured as 80 N, and this reduced to a steady load of 50 N as the process
132 stabilised; these loads correspond to stresses of 99 and 62 MPa respectively, to be compared
133 with the yield strength of 55 MPa according to the manufacturer's data sheet.
134
135 ***PET tube***

136 The outer cylinder was made from the same grade of PET as with the monofilaments
137 described above. Tubes were extruded using the same Killion extruder operating at a screw

speed of 70 rpm and a pressure of 200 bar. The maximum temperature in the extruder was 280 °C and the die head was at 260 °C. Extrusion was through a circular section die of diameter 14mm, with a central internal pin of diameter 4 mm to create the central hole. The haul-off speed was 500 mm min^{-1} and final dimensions were outer diameter 13 mm and inner diameter 6mm.

The tubes were then die-drawn from 1 m lengths through a 30° conical die with an exit diameter of 7 mm. Otherwise, the die-drawing equipment was as used for the drawing of the monofilaments described above. Both the die and oven air temperatures were set at 75 °C. The initial haul-off speed was 40 mm min^{-1} (corresponding to an average strain rate in the die of 0.1 s^{-1}), and was increased during the die-drawing process to reach the maximum draw ratio. The tube's final outer diameter was on average 6.61 mm, corresponding to a draw ratio of 3.9.

PET tube with filaments

An alternative system was studied that consisted of PET monofilaments inside the hollow PET tube samples. This was assembled in its initial isotropic state (see configuration in Figure 1) and then the complete assembly was die-drawn.

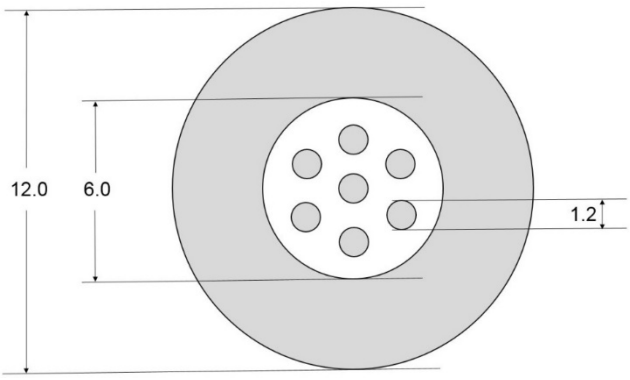

FIGURE 1 Indicative cross-section of multifilament system before drawing. Dimensions in mm

The internal fibres were extruded from Tergal grade T74F9 PET. Extruder and die temperatures were both 280 °C, with extrusion through a 2.5 mm spinneret at a screw speed of 5.4 rpm to achieve a final fibre diameter of 1.2 mm. The outer cylinder was manufactured following the same process described for the PET tube samples.

1 m lengths of tube and filaments were assembled and then die-drawn through a 30° conical die with an exit diameter of 7 mm, following the same procedure as for the PET tube samples. This resulted in a final external diameter of 6.54 mm for the samples, with internal fibres of average diameter 0.57 mm. This corresponds to a draw ratio of 4.0 for the tubes and 4.4 for the internal fibres.

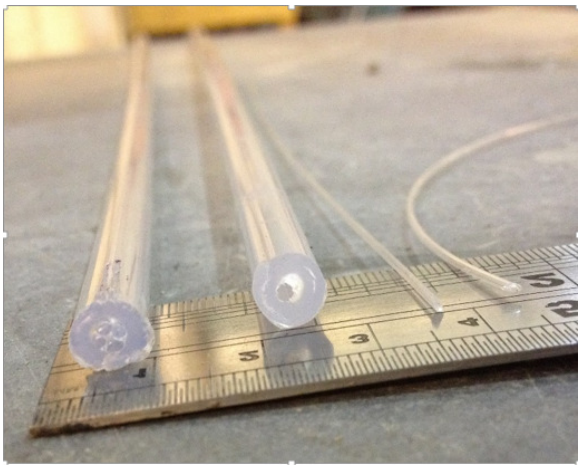

FIGURE 2 Manufactured PET samples, left to right: tube with filaments, tube, solid filament, filament tube

PET strips (commercially available)

The PET strip specimens are commercially available under the name 'shrink tite tape' and were obtained from Cytec.[21] The shrink tite strips used in a previous study were purchased from Aerovac, part of the Umeco Composites group, which was acquired by Cytec in 2012.[21] These strips are made from oriented PET but the manufacturing details are not available.

2.2 Thermal characterisation

For the Dow Lighter C93 material, Modulated Differential Scanning Calorimetry (MDSC) was performed on 5 mg samples of both the unoriented and oriented fibres, corresponding to the two stages of fibre production outlined in the previous section. A TA Instruments Discovery DSC was used, programmed with a mean temperature ramp of 3 °C min^{-1} from 0 °C to 300 °C. In order to decouple the reversible heat flow measurements from non-reversible thermal events a modulation of ±1.0 °C on a period of 1 min was continuously applied to the samples during heating. The glass transition determined from the reversible signal of the MDSC, occurred in the range 70.10 - 77.95 °C for the unoriented sample, with the upper end of the range in good agreement with the manufacturer's value of 78.0 °C. Further unmodulated testing at a ramp of 2°C min^{-1} established that crystallinity was in the range 9 – 12%. The results of the measurements on the oriented fibre will be discussed in section 3.1.

2.3 Equipment and test specimen preparation

Thermal triggering was achieved by direct heating in an Instron environmental chamber. Each sample was clamped within steel friction grips, which were subjected to preliminary testing to ensure there was no significant slippage of the samples during activation.

A diagram of the rig used to test each sample is shown in Figure 3. The rigs were connected to a 5kN load cell and three thermocouples were placed on the samples, denoted T1, T2 and T3. The load cell and thermocouples were attached to a data logger set to record at a rate of 1 Hz. Each sample was pre-loaded manually to a stress of 2 MPa to ensure that there was no slack which would affect the shrinkage results.

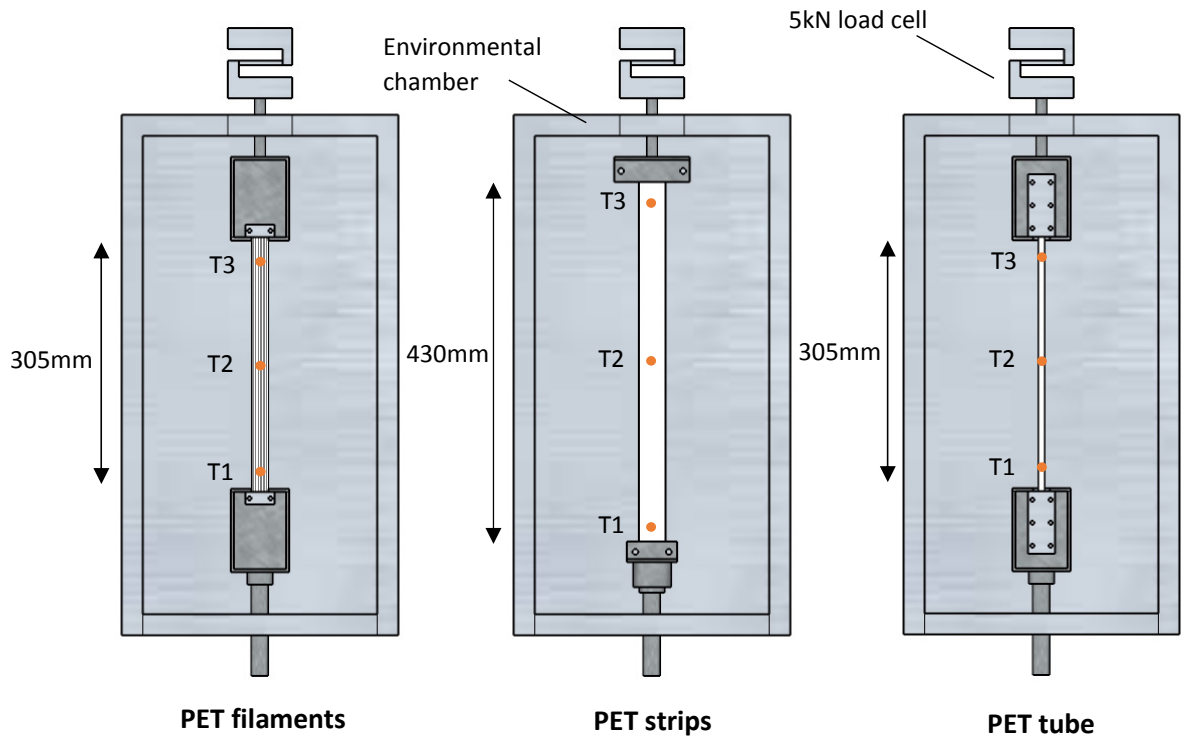

198

199 **FIGURE 3 Environmental chamber rig setup for each sample type**

200

201

202 **2.4 Test procedure**

203 The samples used within each test are detailed in TABLE 1. The testing procedures used were

204 as follows:

205

206 ***Shrinkage stress at 90°C (Test Series 1, TS1)***: The samples were heated to 90 °C in the

207 environmental chamber and left for a soak time of 1 hr. The environmental chamber was then

208 turned off and the sample allowed to cool back to room temperature. Load and temperature

209 were measured continuously at a sample rate of 1 Hz. The *strip* and *filament* samples were

210 tested in bundles of 10, whilst the *tube* and *tube with filaments* were tested as single samples.

211

212 ***Temperature-shrinkage profile (Test Series 2, TS2)***: The samples were heated to 60 °C within

213 an Instron environmental chamber and held at a constant temperature for 30 mins (soak
214 time). The temperature was then increased in 10 °C increments, keeping the soak time
215 constant at each increment, up to 140 °C. The environmental chamber was then turned off
216 and the sample allowed to cool back to room temperature. Load and temperature were
217 measured continuously at a sample rate of 1 Hz. The *strip* and *filament* samples were tested
218 in bundles of 10, while the *tube* and *tube with filaments* were tested as single samples.
219
220 ***Free shrinkage (Test Series 3, TS3):*** Samples of original length 305 mm were placed within
221 the environmental chamber and heated to 90 °C for 18 hrs. They were then allowed to cool
222 to room temperature and their final lengths recorded.
223
224 The above test series were used to select a form of PET for further investigation. *Solid filament*
225 and *filament tube* samples, having exhibited greater shrinkage stresses than the PET *strips*,
226 were then subjected to additional testing along with the strips to compare their mechanical
227 properties.
228
229 ***Tensile strength tests (Test Series 4. TS4):*** Individual PET *solid filament*, *filament tube* and
230 *strip* samples were subjected to tensile loading in a Zwick Z100 tensile testing machine.
231 Loading was displacement-controlled. For the PET *strips*, loading rates of 0.05 mm s^{-1}, 0.1 mm
232 s^{-1} and 0.2 mm s^{-1} were used to check the effect of loading rate. For the *solid filament and*
233 *filament tube* samples, a 0.1 mm s^{-1} rate was used. Loading was continued until the samples
234 failed. PET *strip* samples, which had been activated (heated to 90 °C for 1 hr), were also tested
235 for comparison. Load and displacement were measured continuously at a sample rate of 1
236 Hz.

Effect of temperature on Young's modulus (Test Series 5, TS5): Using a Dartec tensile testing machine and an Instron environmental chamber, individual PET *solid filament* samples and PET *strips* in stacks of four were held at a constant load, equivalent to a stress of 10 MPa, while the temperature was increased in increments of 10 °C from 30 °C to 130 °C with a soak time of 5 mins. At each temperature increment, a cyclic stress with amplitude 10 MPa was applied to the sample. Three rates of stress were used: 3.4 MPa s^{-1}, 0.34 MPa s^{-1} and 0.034 MPa s^{-1}. Load and displacement was measured continuously at a sample rate of 10 Hz and used to calculate Young's modulus at each temperature.

3 RESULTS AND DISCUSSION

3.1 Peak shrinkage stress in TS1 samples

In all of the TS1 samples, the peak restrained shrinkage stress, during the heating phase, occurred when the environmental chamber temperature was 90 °C. In some cases, higher stresses were observed upon cooling, which is thought to be due to the thermal contraction of the steel rig. This issue is discussed below. The peak stress results are shown in TABLE 2.

TABLE 2 Peak restrained shrinkage stress results

	Restrained shrinkage stress for TS1 specimens at 90 °C (MPa)			
Polymer	Highest	Lowest	Average	CoV (%)
Strips	24.93	23.03	24.02	3.97
Solid filament	41.50	36.98	38.58	6.56
Filament tube	43.33	38.67	40.93	5.7
Tube	23.10	-	23.10	-
Tube with filaments	17.01	-	17.01	-

As can be seen from the stress results, the highest average shrinkage stress was observed in the PET *filament tube* samples, with the lowest stress exhibited by the *tube with filaments* specimens. Both of the *filament* samples produced significantly higher stresses than either the *strips* or the larger PET *tubes*. The trend in these results is supported by the fact that the degree of crystallisation reduces with the cross-sectional area of a sample and that crystallisation of the polymer matrix reduces the shape recovery potential of shape memory polymers by increasing the material's resistance to shrinkage.[22]

In addition, since the shrinkage stress is correlated to the stored energy within the polymer, maximising the force used to draw the filaments - through the use of a high drawing rate (1m min^{-1}) - further contributed to the increased shrinkage stresses in the *filament* samples relative to those of the *tube* samples (40 mm min^{-1} initial). The *tube with filament* samples exhibited similar shrinkage behaviour to the *tube* samples, indicating that the maximum stress seems to be limited by the external tube.

The graphical results of the restrained shrinkage stress at 90°C for all samples can be seen in Figure 4. In all cases, heating to 90 °C produces a rapid increase in stress followed by a plateau. Upon cooling, there was a subsequent increase of 2-3 MPa in all but one test set (i.e. 4b).

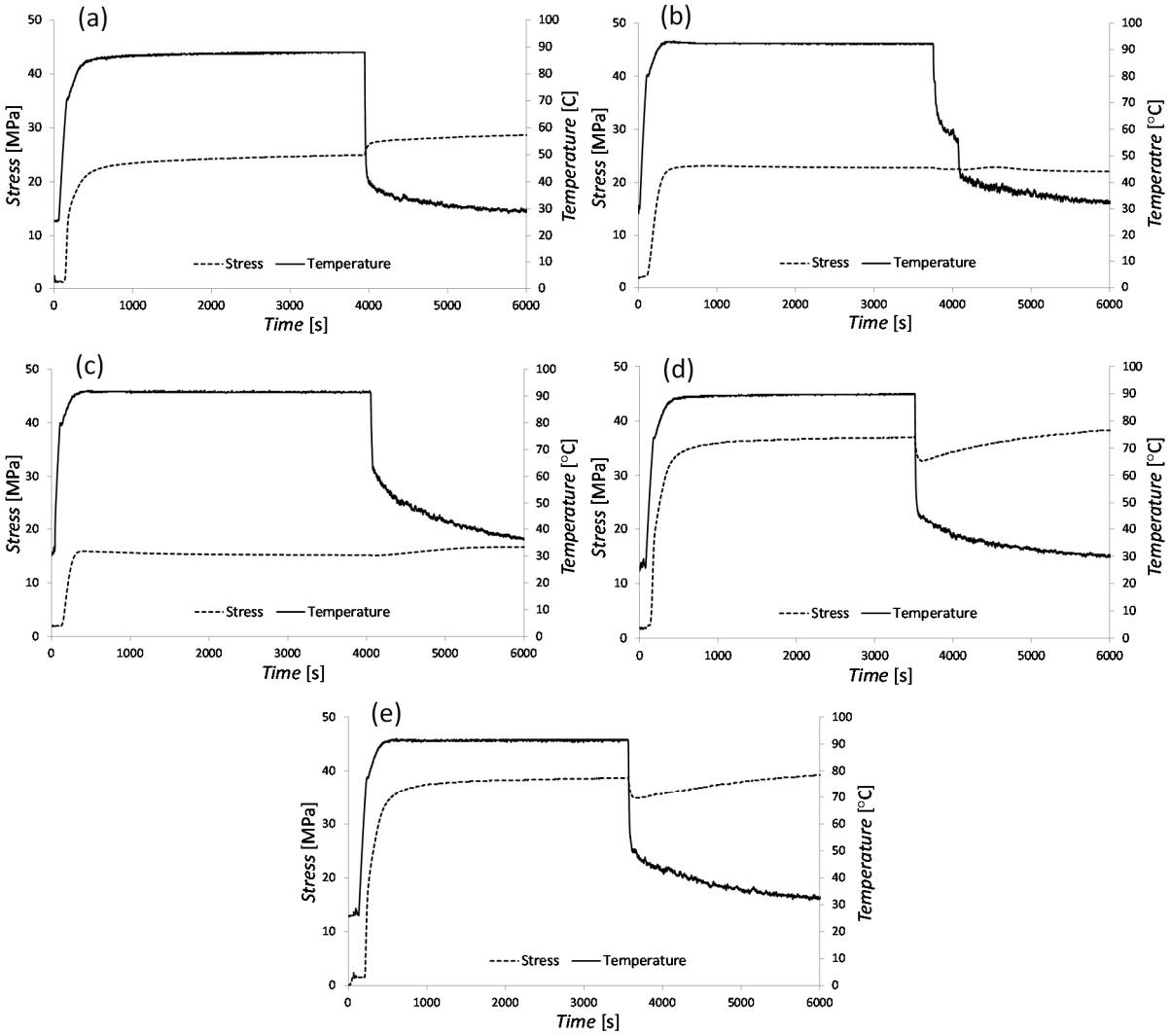

273

274 **FIGURE 4 Restrained shrinkage stress at 90°C for (a) Strips; (b) Tube; (c) Tube with filaments; (d) Solid**
275 **filaments & (e) Filament tube. Typical results graphs shown for samples with repetitions.**

276

277 This increase in stress can be attributed to the contraction of the steel rig used to transfer the
278 shrinkage stress of the PET to the load cell. This was later confirmed in some separate tests in
279 which samples were heated using a system of embedded wires. This system caused no
280 appreciable change in temperature in the steel rig. In this case, there was no increase in the
281 polymer stress during the cooling phase.

282 It is noted that the peak stress observed at 90 °C in the PET *strip* samples is lower than the
283 30-35 MPa found in previous study.[10] This variation may be due to manufacturing process

changes since the original tests were undertaken and is discussed in more detail in section 3.5.

The *filament* samples produced an initial drop in stress upon cooling, which was not observed in the other samples or in previous shrinkage experiments on PET *strip* samples. The testing temperature of 90 °C is well above T_g (78 °C), so we may assume that the shrinkage stress is entropic and is proportional to *NkT*, where N is the number of molecular chains per unit volume, k is Boltzmann's constant, $\text{and } T$ is the absolute temperature.[23] Thus, the stress drop is expected to be directly related to the drop in *T*. However, during the course of the stress drop the temperature falls below T_g, whereupon the stress will cease to be proportional to *NkT* and will attain a constant value as the molecules become confined within the structure. On this basis we would expect the ratio of stresses before and after the stress drop to be T_{test}/T_g, where T_{test} is the testing temperature and both temperatures are expressed in degrees Kelvin.

To assess quantitatively the validity of this argument, we must decide upon the appropriate value of T_g in the context of a cooling oriented polymer. Values for PET both in isotropic form and oriented to a draw ratio of 4, using differential scanning calorimetry (DSC) and dynamic mechanical thermal analysis (DMTA), have been found to exhibit significant differences.[24] The T_g was measured as around 80 °C for isotropic material, with the glass transition process starting at 70 °C; however, in oriented form the onset of glass transition was lower by 15 °C, with the T_g correspondingly lower. We have investigated the effects of molecular orientation on the Dow Lighter material by TDSC, as described above. The measurements apply most specifically to the results of Figure 4(d).

For oriented fibre, it was possible to detect in the non-reversible signal an exothermic peak commencing at a temperature of 72.906 °C with a peak value occurring at 86.637 °C (see Figure 5). This we interpret as related to relaxation of the residual stresses, which would correspond to the onset of shrinkage stresses for a restrained specimen. This is consistent with the effectiveness of the test temperature of 90 °C.

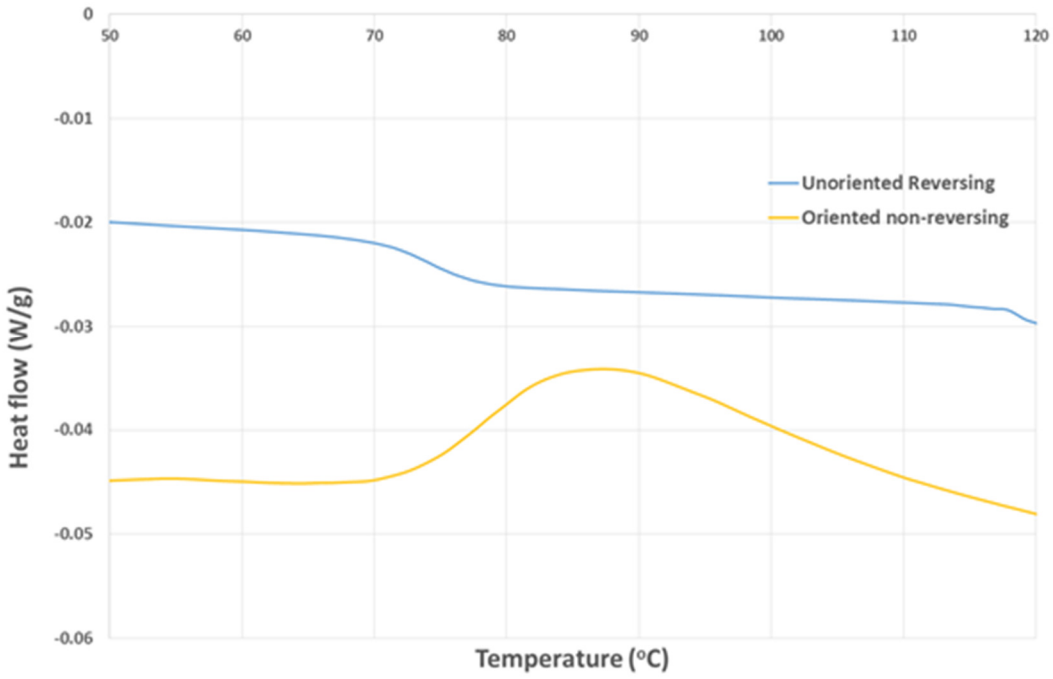

FIGURE 5 Results from TDSC testing on oriented fibre material.

The glass transition was not found to significantly differ from that of the unoriented material, occurring in the range 70 - 78 °C. This gives a range of values of the ratio T_{test}/T_g of $1.03 < T_{test}/T_g < 1.05$, to give a maximum stress drop of 1.6 MPa from the observed maximum 35 MPa in Figure 4(d). This compares with an observed drop of 4.3 MPa. This is a significant discrepancy, for which two factors may be relevant. First, in the shrinkage experiments, the polymer is restrained while cooling, whereas it is free to contract in the TDSC tests, possibly leading to different Tg values. Secondly, the temperatures in the restrained shrinkage tests

recorded are air temperatures, which during cooling will in general be higher than those obtaining at the core of the fibre bundle, leading to a longer time above T_g.

3.2 Temperature-shrinkage profiles in TS2 specimens

The restrained shrinkage stress recorded at each temperature interval has been plotted as temperature-shrinkage profiles in Figure 6.

It is observed for the PET *strip* samples that the shrinkage stress starts to increase significantly when the temperature exceeds 70 °C, reaching a peak of 28.7 MPa at 130 °C. Thereafter, the stress starts to fall as the temperature increases further, which is consistent with the findings from previous tests on similar materials.[10,11]

The *solid filament* and *filament tube* samples exhibited stress peaks of 41.8 MPa and 42.9 MPa respectively, both at 110 °C.

The PET *tube* and *tube with filaments* samples showed peak stresses of 18.3 MPa and 16.2 MPa respectively at the lower temperature of 90 °C. It is not clear why the peak activation temperature of the *tubes* are lower than the *filament* samples, although this could be related to the lower drawing temperature of 75 °C in comparison to the 80 °C of the *filament* samples and the different crystalline phase relative volumes.

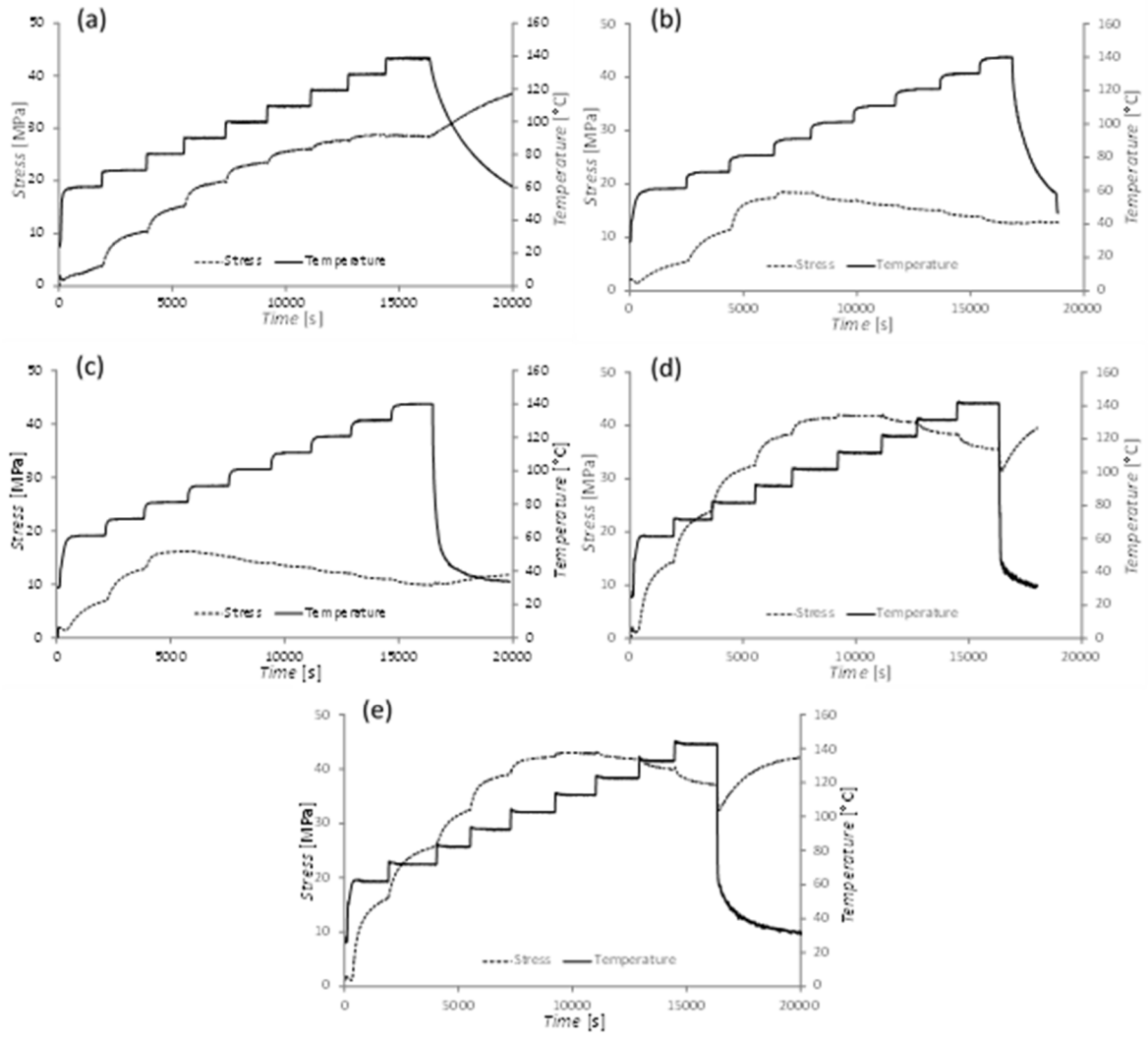

FIGURE 6 Temperature-shrinkage profiles for (a) Strips; (b) Tube; (c) Tube with filaments; (d) Solid filaments and (e) Filament tube.

The low peak shrinkage stress measured in the *tube with filament* samples may be associated with a degree of relative slip between the external tube and the inner filaments, both along the length of the specimens and at the grips. Such slip behaviour would cause a reduction in the contribution of the filaments to the overall composite shrinkage force and therefore to the mean shrinkage stress.

All samples show a drop in shrinkage stress beyond the peak activation temperature. This is believed to be caused by the reduction in yield stress that accompanies an increase in

352 temperature, as predicted by Eyring's model,[23] which becomes very significant beyond 140
353 °C. In addition to this effect is the fact that at these temperatures the polymer has released
354 most of the energy stored during the drawing process.

355

356 **3.3 Free shrinkage tests in TS3 specimens.**

357 Results of the free shrinkage experiments, presented in TABLE 3, show that the shrinkage at
358 90 °C observed for all manufactured samples exceeds that of the PET *strips*. This trend is
359 attributed to the relatively high draw ratio used in the manufacture of the former specimens.
360 The difference in draw rate between the *filament* samples and the *tube* samples does not
361 seem to have altered the free shrinkage properties.

362 **TABLE 3 Free shrinkage at 90°C results**

Sample type	Number of samples	Draw ratio	Draw rate (mm s^{-1})	Average shrinkage (% length)
Strips	10	unknown	unknown	1.6
Solid filament	10	4.0	1000	5.0
Filament tube	10	4.0	1000	4.7
Tube	1	3.9	40 (initial)	5.2
Tube with filaments	1	4.0 (tube) 4.4 (int. filaments)	40 (initial)	7.2

363

364 The *solid filament*, *filament tube* and *tube* samples all produced similar free shrinkage results,
365 whilst the shrinkage of the *tube with filaments* sample was 2 % greater than any of the other
366 specimens. This contrasts with the peak shrinkage results in which the *tube with filaments*
367 sample produced the lowest restrained shrinkage stress. Free shrinkage in this case seems to
368 have no correlation to the restrained shrinkage stress or to the draw rate.

369 It is noted that the free shrinkage strain is opposite in sign to conventional thermal expansion.
370 The coefficient of thermal expansion of these PET materials at 20°C varies from 60 to 80×10^{-6}/°C , which –in the absence of any shape memory or softening effects- would equate to an
371
372 total expansion strain of approximately 0.5% over the temperature range 25 to 90 °C.

373

374 **3.4 Tensile strength tests in TS4 specimens**

375 The results of the tensile strength tests are given in TABLE 4. The rate of loading has little
376 effect on the tensile stress of the samples at failure. Furthermore, the tensile strengths of the
377 activated PET *strip* samples are similar to those of the non-activated *strips*. This indicates that
378 activating the polymers does not weaken the material in tension, which is beneficial in the
379 context of their use within the concrete tension zone.

380 **TABLE 4 Tensile strength test results**

Sample	Type	Rate (mm s^{-1})	Stress at failure (MPa)	Strain at failure (%)	Avg. tensile strength (MPa)	CoV (strength) (%)	Average strain at failure (%)
1	PET strip	0.1	186.5	14.6			
2	PET strip	0.1	187.0	18.3	189.2	1.9	20.1
3	PET strip	0.1	194.2	27.5			
4	PET strip	0.2	188.7	15.0			
5	PET strip	0.2	186.8	12.4	187.3	0.5	13.2
6	PET strip	0.2	186.4	12.3			
7	PET strip	0.05	177.6	9.7	179.7	1.2	10.8
8	PET strip	0.05	181.9	11.9			
9	PET strip - heated	0.1	188.9	11.4			
10	PET strip - heated	0.1	178.8	7.7	185.0	2.4	10.5
11	PET strip - heated	0.1	187.3	12.5			
12	PET filament solid	0.1	305.2	6.7			
13	PET filament solid	0.1	309.9	7.2	304.9	1.4	6.6
14	PET filament solid	0.1	300.0	6.0			
15	PET filament tube	0.1	317.8	7.8			
16	PET filament tube	0.1	305.7	6.9	308.5	2.2	7.4
17	PET filament tube	0.1	302.1	8.0			

381

These results show that the solid and tube filament samples exhibit significantly higher tensile strengths than the strips. Lower 'strain at failure' results indicate an increased stiffness in the *filament* samples. These results, along with the restrained shrinkage stress values, suggest that the *strip* samples are probably drawn to a lower draw ratio than the filaments. This deduction is supported by the well-established trend that stiffness in drawn polymers increases with the draw ratio.[23] This also agrees with the free shrinkage results, since a lower draw ratio for the strip samples would result in a reduced degree of orientation and therefore a smaller free shrinkage strain than measured in the other samples.

The tensile tests results indicate that the two *filament* types, solid and tube, have very similar tensile strength properties.

3.5 Effect of temperature on Young's modulus in TS5 specimens

The results of the Young's Modulus (YM) tests on the PET *solid filaments* and the PET *strips* are shown in Figure 7. As the PET *solid filament* and *tube filament* samples had exhibited almost identical shrinkage and tensile properties, having been subjected to identical methods of manufacture, YM experiments were carried out only on the *solid filament* samples.

At each temperature, Young's modulus (E_{ap}) was calculated from the loading and unloading portions of three 10 MPa stress cycles and averaged. Both the stress and strain were assumed to be uniaxial, with strain being computed from the change in displacement over the initial gauge length, and stress from the applied load divided by the undeformed area.

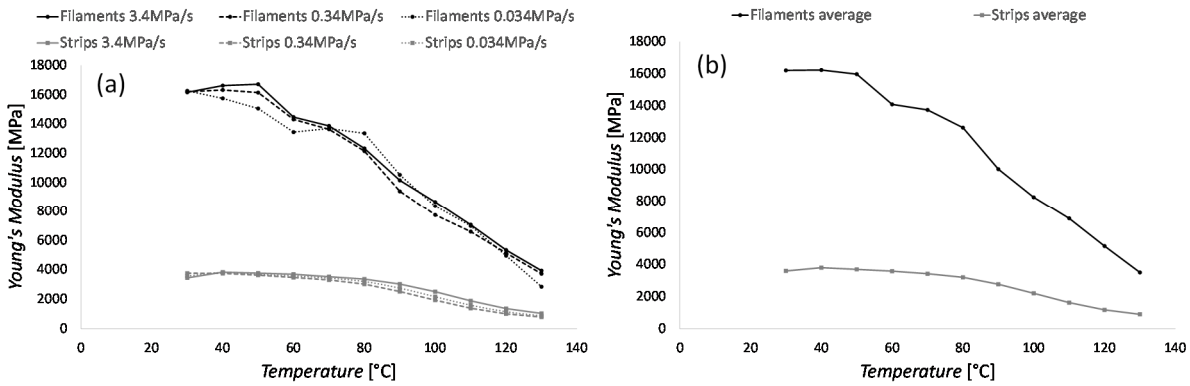

402

403 **FIGURE 7 Young's Modulus with temperature for drawn PET solid filaments and PET strips (a) using 3.4 MPa**
404 **s^{-1}, 0.34 MPa s^{-1} and 0.034 MPa s^{-1} load cycles, and (b) as an average over all load cycles**

405

406 The data presented in Figure 7 show that the E_{ap} value is relatively insensitive to the stress
407 rate for both sets of specimens. A previous study by the authors[10], conducted on a similar PET
408 material, showed a slightly stronger (although still modest) stress-rate dependency. These
409 earlier data where interpreted in the light of an SLS-based (Standard Linear Solid) rheological
410 model in such a way that viscosity values and strain-rate independent low and high
411 temparture Young's moduli were extracted from the data. However, in the present case, the
412 stress-rate dependency was considered too weak to warrant such an analysis and therefore
413 only the average E_{ap} values are presented. It is also noted that other authors have suggested
414 that the best way to compute Young's moduli is to use the slope of stress vs. strain response
415 in the early unloading stages of each cycle.[25]

416 The stress excursion of 10MPa (3 to 5% of the unheated tensile strengths) is greater than the
417 values used in some previous studies[10] but the consistency of the results and linearity of the
418 unloading-reloading cycle suggest that this stress change value was reasonable.

419

For both polymer forms, there is a clear reduction in E_{app} with increasing temperature. This is expected because the slower the testing rate the greater will be the contribution to strain changes from viscous effects. Furthermore, as the melting point of the polymer is approached the polymer softens. The results show a clear drop in E_{app} once the glass transition temperature of around 70 °C has been reached, with continuing loss of stiffness to 130 °C.

The *filament* samples produced significantly higher E_{app} values than the *strips*, which is consistent with the findings from the tensile strength tests. We note that the strip results presented here are significantly different from those obtained in the previous study,[10] where higher E_{app} results were observed for the commercially available *strips*, around 6000 MPa at 30 °C compared to below 4000 MPa measured for the current samples. This difference may be due to a change in the processing of the *strip* samples during manufacture, which would also explain the differences in shrinkage stress results. These findings suggest that the commercially available strips were previously drawn to a higher draw ratio, leading to higher orientation and stiffness in the samples tested in previous studies.[10,11]

3.6 General Discussion

Neither long-term relaxation, nor its creep counterpart, were considered in the present work. The Cardiff team[26] has previously investigated the relaxation of shrinkage stresses over a 6 month period for Shrink tite PET samples.[26] The main conclusions from this study were that the long-term relaxation of the restrained shrinkage stress in drawn PET is relatively small, i.e. 2 to 3 % of the peak stress, and the majority of stress loss occurs over the first 12 days after activation. The same conclusions cannot be transferred to other polymers.[25]

442 The work reported in this paper concentrated on peak shrinkage stresses but, as with all
443 prestress systems, there will be some losses due to concrete creep and shrinkage, as well as
444 relaxation of the tendons, although the latter losses are likely to be small for reasons
445 explained above. The present system is targeted at closing early-age cracks and promoting
446 the conditions for early-age autogenous healing; therefore, long-term losses are of secondary
447 importance.

448

449 **4 CONCLUSIONS**

450 Experiments undertaken to test the shrinkage stress of PET samples of varying cross-section
451 and processing histories has resulted in the development of a high shrinkage PET filament for
452 use within a concrete crack closure system.

453 It is concluded from our tests that the restrained shrinkage stress potential in drawn PET
454 samples increases with increasing draw ratio, increasing draw rate and decreasing specimen
455 cross-section. The restrained shrinkage stresses achieved in a series of drawn PET *filament*
456 specimens, manufactured at Bradford University, were significantly larger than those
457 obtained from the commercially available PET *strips* used in previous experiments.[10,11,18] The
458 shrinkage stress measured was also higher than that produced by PET *tube* and *tube with*
459 *filament* samples subjected to similar die-draw processing. This is attributed to a higher draw
460 rate resulting in a greater amount of stored energy within the filament samples.

461 The PET *filaments* exhibited a stress drop upon cooling not previously observed for drawn
462 polymer samples. This is believed to be due to the drop in stress caused by a reduction in the
463 entropic elasticity with falling temperature (for T below T_g) being greater than the increase in

stress from restrained thermal contraction. It is concluded that the balance between these mechanisms is different in the PET *filaments* from that in the other materials tested.

This programme of work has succeeded in developing a PET form which produces approximately double the restrained shrinkage stress potential, and 1.7 times the tensile strength, of commercially available *strip* samples. The PET *filament*, having exhibited the largest shrinkage stress potential, has been subsequently used in a series of crack closure experiments in concrete structural elements.

ACKNOWLEDGEMENTS

Thanks must go to the EPSRC for their funding of the Materials for Life (M4L) project (EP/K026631/1) and to Costain Group PLC. for their industrial sponsorship of the project and author.

REFERENCES

1. W. M. Huang & Y. Zhao & C. C. Wang & Z. Ding & H. Purnawali & C. Tang & J. L. Zhang.. A Thermo/chemo-responsive shape memory effect in polymers: a sketch of working mechanisms, fundamentals and optimization, Journal of Polymer Research, Vol. 19, No. 9, **2012**, 9952
2. Xie, T., *Polymer*, **2011**, 52, 4985.
3. Huang, W. M.; Ding, Z.; Wang, C. C.; Wei, J.; Zhao, Y.; Purnawali, H., *Materials Today*, **2010**, 13, 54.
4. Sweeney, J.; Bonner, M.; Ward, I. M., *Journal of the Mechanical Behavior of Biomedical Materials*, **2014**, 37, 12.
5. Meng, Q.; Hu, J., *Composites Part A: Applied Science and Manufacturing*, **2009**, 40, 1661.
6. Xu, J.; Song, J., *Biomedical Engineering - Frontiers and Challenges*, **2011**.
7. Sun L, Huang WM, Wang CC, Zhao Y, Ding Z, Purnawali H. Optimization of the Shape Memory Effect in Shape Memory Polymers. Journal of Polymer Science Part A Polymer Chemistry, 49, 3574-3581 (2011).
8. Miaudet, P.; Derre, A.; Maugey, M.; Zakri, C.; Piccione, P. M.; Inoubli, R.; Poulin, P., *Science*, **2007**, 318, 1294.
9. Alves, N. M.; Mano, J. F.; Balaguer, E.; Meseguer Dueñas, J. M.; Gomez Ribelles, J. L., *Polymer*, **2002**, 43, 4111.
10. Dunn, S. C.; Jefferson, A. D.; Lark, R. J.; Isaacs, B., *Journal of Applied Polymer Science*, **2011**, 120, 2516.
11. Jefferson, A.; Joseph, C.; Lark, R.; Isaacs, B.; Dunn, S.; Weager, B., *Cement and Concrete Research*, **2010**, 40, 795.
12. Neuser S, Michaud V, White SR. Improving solvent-based self-healing materials through shape memory alloys. Polymer, 53:370-378, (**2012**).

13. Kirkby EL, Michaud VJ, Månson JAE, Sottos NR, White SR. Performance of self-healing epoxy with microencapsulated healing agent and shape memory alloy wires. Polymer, 50: 5533-5538, (**2009**).
14. Kirkby EL, Rule JD, Michaud VJ, Sottos NR, White SR, Månson JAE. Embedded shape-memory alloy wires for improved performance of self-healing polymers. Advanced Functional Materials,18: 2253-2260, (**2008**).
15. Li G, Ajisafe O, Meng H. Effect of Strain Hardening of Shape Memory Polymer Fibers on Healing Efficiency of Thermosetting Polymer Composites. Polymer, 54: 920-928, (**2013**).
16. Li G, Meng H, and Hu J. Healable Thermoset Polymer Composite Embedded with Stimuli-responsive Fibers. Journal of the Royal Society Interface, 9:3279-3287, (**2012**).
17. Li G and Zhang P. A self-healing particulate composite reinforced with strain hardened short shape memory polymer fibers. Polymer, 54: 5075-5086, (**2013**).
18. Dunn, S. C.; Jefferson, A. D.; Lark, R. J.; Isaacs, B., *Journal of Applied Polymer Science*, **2011**, 120, 2516.
19. Hazelwood, T.; Jefferson, A. D.; Lark, R. J.; Gardner, D. R., *Engineering Structures*, **2015**, 102, 176.
20. Coates, P. D.; Ward, I. M., *Polymer Engineering and Science*, **1981**, 21, 612.
21. CYTEC, Cytec Solvay Group http://www.cytec.com; (accessed April 2016).
22. Mody, R.; Lofgren, E. A.; Jabarin, S. A., *Journal of Plastic Film and Sheeting*, **2001**, 17, 152.
23. Ward, I. M.; Sweeney, J., Mechanical properties of solid polymers; Wiley: Chichester, UK, **2013**.
24. Bartolletta, A.; Di Marco, G.; Farsaci, F.; Lanza, M.; Pieruccini, M., *Polymer*, **2003**, 44, 5771.
25. X. L. Wu, W. M. Huang, H. X. Tan to Characterization of shape recovery via creeping and shape memory effect in ether-vinyl acetate copolymer (EVA), Journal of Polymer Research, Vol. 20, **2013**, 150).
26. T. Hazelwood, A. D. Jefferson, R.J. Lark, D. R. Gardner **2014**. Long-term stress relaxation behavior of predrawn poly(ethylene terephthalate). Journal of Applied Polymer Science 131(23)